Petroleum Science 22 (2025) 1200–1213

Contents lists available at ScienceDirect

Petroleum Science

journal homepage: www.keaipublishing.com/en/journals/petroleum-science

Original Paper

Experimental investigation into CO_2 huff-n-puff in low-permeability heavy oil reservoirs: Role of fractures

Di Zhu [a,b], Bin-Fei Li [a,b], Lei Zheng [c], Maen M. Husein [d,*], Zheng-Xiao Xu [a,e], Bo-Liang Li [a,b], Zhao-Min Li [a,b,**]

[a] State Key Laboratory of Deep Oil and Gas, China University of Petroleum (East China), Qingdao, 266580, Shandong, PR China
[b] School of Petroleum Engineering, China University of Petroleum (East China), Qingdao, 266580, Shandong, PR China
[c] NO.1 Gas Production Plant, Southwest Oil & Gas Company, SINOPEC, Deyang, 618000, Sichuan, PR China
[d] Department of Chemical & Engineering, University of Calgary, Calgary, T2N 1N4, AB, Canada
[e] School of Petroleum and Natural Gas Engineering, Changzhou University, Changzhou, 213164, Jiangsu, PR China

ARTICLE INFO

Article history:
Received 11 June 2024
Received in revised form
18 November 2024
Accepted 20 November 2024
Available online 22 November 2024

Edited by Yan-Hua Sun

Keywords:
Low-permeability reservoir
Heavy oil
CO_2 HnP
Unpropped fracture
Fracture aperture

ABSTRACT

Low-permeability heavy oil reservoirs are characterized by poor flowability, generally mandating hydraulic fracturing to commence production. CO_2 huff-n-puff in fractured reservoirs is an effective enhanced oil recovery method. This paper uses nuclear magnetic resonance imaging to elucidate the role of propped and unpropped fractures on CO_2 huff-n-puff in cores under different confining pressures. In presence of fractures, significant improvement in the rate of early stage oil recovery is observed, up to 0.255 mL/min. Fractures enlarge the contact area between CO_2 and the heavy oil, hence improve CO_2 dissolution and oil flowability. Fractures improve oil recovery from micropores, small pores, and mesopores, as well as reduce CO_2 consumption ratio. The oil recovery factor in propped fractures is significantly higher than that in unpropped fractures, and with higher oil recovery from small pores and mesopores. The oil recovery in fractured cores noticeably decreases with increasing confining pressure. The extent of fracture closure increases and the matrix pore throats compress under pressure leading to lower apparent permeability. The decrease in oil recovery factor is more pronounced in unpropped fractured cores. A relationship between the apparent permeability of the fracture aperture is derived based on the modified cubic law of percolation to quantitatively characterize the fracture. Additionally, both the reduction in heavy oil viscosity and the increase in experimental temperature and pressure can improve the CO_2 huff-n-puff oil recovery factor in fractured cores.

1. Introduction

Low-permeability heavy oil reservoirs are abundant and contain large reserves (Li et al., 2024a; Wan et al., 2020; Wang et al., 2023), hence serve as an important alternative for late stage oil field development. However, in addition to their low-permeability, these reservoirs are impacted by deep burial and high fluid viscosity. Accordingly, low-permeability reservoirs display production characteristics of high initial rates followed by a rapid decline (Cao et al., 2021; Sun et al., 2023; Zhu et al., 2023; Zhou et al., 2024). These reservoirs often contain thin interbedded layers of loose sandstones and low-permeability tight sandstones. Most low-permeability heavy oil reservoirs require reliable reservoir stimulation leading to well-planned hydraulic fracturing in order to increase their permeability (Altawati et al., 2022; Wei et al., 2020a; Zhang et al., 2021a; Li et al., 2024b).

Hydraulic fracturing induces two main types of fractures: tensile fractures and shear misalignment fractures (Cheng and Milsch, 2021; Lu et al., 2020; Ojha et al., 2024). Tensile fractures are the main and branch fractures. They can be propped by proppant to maintain open fractures when fracturing is complete. Shear misalignment fractures are relatively dislocated induced unpropped fractures that cannot be completely closed owing to geostresses. The fracture network in the reservoir after hydraulic fracturing consists of propped fractures near the wellbore and unpropped fractures

* Corresponding author.
** Corresponding author.
E-mail addresses: mhusein@ucalgary.ca (M.M. Husein), lizhm@upc.edu.cn (Z.-M. Li).

https://doi.org/10.1016/j.petsci.2024.11.015
1995-8226/

farther from the wellbore (Ahamed et al., 2021; Jia et al., 2022; Lu et al., 2022). Laboratory studies have shown that the conductivity of unpropped fractures is numerically on the same order of magnitude as that of fractures with single-layer proppant, and even under high closure stress, unpropped fractures can still contribute significantly to oil recovery (Ribeiro et al., 2017). Unpropped fractures are primarily formed through shear slippage in the reservoir during the fracturing process. As the slippage increases, the conductivity of unpropped fractures gradually improves (Fredd et al., 2001). However, excessive slippage may reduce the roughness of the fracture walls and potentially lead to closure of the fractures. Additionally, under the influence of closure stress, the deformation and closure of unpropped fractures significantly alter the internal flow regions and reduce the fracture conductivity (Cook, 1992; Kamali and Pournik, 2016; Pyrak-Nolte and Morris, 2000), thus weakening the fracturing stimulation effect. Consequently, unpropped fractures provide a certain level of conductivity. However, the mechanisms for maintaining this conductivity as well as the impact of fracture opening and closing trends on fluid flow within the reservoir still need further investigation.

The deep burial of low-permeability heavy oil reservoirs reduces oil recovery and increases operational costs, especially for conventional thermal production methods. CO_2 huff-n-puff (HnP) cold production is regarded as a viable heavy oil production technique, notable for its minimal resource consumption, scalability, and effectiveness. CO_2 can substantially reduce the viscosity of heavy oil, thereby improving reservoir fluid flowability (Li et al., 2020a; Zhou et al., 2018, 2019b, 2022). Meanwhile, greenhouse gas emission reduction through capturing and trapping CO_2 is a growing practice (Li et al., 2022; Melzer, 2012; Zhu et al., 2024). The CO_2 HnP process, combined with multistage hydraulic fracturing technique, not only overcomes the challenges of low injectivity of the fluid medium in low-permeability reservoirs but also effectively prevents the occurrence of gas channeling (Lv et al., 2024; Wei et al., 2020b). Compared to conventional water-based EOR methods, CO_2 HnP can address the water channeling issues encountered during water flooding after fracturing, while also resolving the high costs and strict application conditions associated with polymer flooding or foam flooding. In particular, CO_2 HnP technology has yielded favorable results in both laboratory experiments and oil field production (Bao et al., 2023; Zhang et al., 2024). Laboratory experiments found that the matrix oil recovery factor for fractured core ranged from 50.5% to 74.3% through multiple cycles of CO_2 HnP experiments, while for fracture-free cores, the oil recovery factor ranged from 18.5% to 31.2% (Zhu et al., 2021). Additionally, in a numerical simulation of CO_2 HnP in the Bakken reservoir, the oil recovery factor increased by more than 9% after 30 years of production (Yu et al., 2014). Similarly, after multiple cycles of CO_2 HnP in the Jimsar reservoir, the oil recovery increased by 9.4% (Cao et al., 2023).

The primary mechanisms of enhance oil recovery (EOR) of CO_2 HnP in heavy oil reservoirs are viscosity reduction and oil swelling. The higher the initial viscosity of the heavy oil, the greater the reduction in viscosity through CO_2 dissolution (Khatib et al., 1981; Sayegh and Maini, 1984). In addition, the dissolution of CO_2 in heavy oil induces volumetric expansion, which increases the pore pressure, thereby improving the driving force and facilitating the recovery of residual oil (Tharanivasan et al., 2006). Moreover, oil swelling enhances the oil saturation leading to an increase in oil relative permeability, which in turn enhances the oil phase fractional flow during the production stage (Grogan and Pinczewski, 1987). CO_2 diffusion is also a critical EOR mechanism for CO_2 HnP in heavy oil reservoirs. Although the diffusion coefficient of CO_2 in heavy oil reservoirs is lower than in tight oil reservoirs, CO_2 diffusion still plays an important role during the soaking stage of the HnP process (Yuan et al., 2017a). During the injection stage of HnP, CO_2 injected into the reservoir interacts only with the heavy oil near the wellbore. However, in the subsequent soaking stage, CO_2 gradually diffuses and dissolves into the heavy oil at more distant locations. This process supplements viscosity reduction and oil swelling, thereby expands the sweep area of CO_2 and enhances heavy oil recovery (Huang et al., 2016; Yuan et al., 2017b). Dissolved CO_2 drives oil recovery when pressure drops during the production stage through foamy oil flow (Liu et al., 2013; Or et al., 2016; Sheng et al., 1999).

Literature on the application of CO_2 HnP in heavy oil reservoirs primarily focuses on the EOR mechanisms. Additionally, there are numerous studies of the impact of fracture geometry on CO_2 HnP efficiency in low-permeability or tight reservoirs, including experimental studies of wire-cut fracture geometry and numerical simulation studies of fracture geometry. Larger fracture length and width are more favorable for the CO_2 HnP process because they provide more contact area with the reservoir, allowing CO_2 to diffuse into a larger portion of the reservoir and resulting in a higher recovery factor (Yu et al., 2015). Through CO_2 HnP experiments on cores with different intersection angles of the fracture, it was found that the core with a horizontal fracture had the highest oil recovery. When the intersection angles of the core fractures were 90°, 68°, and 43°, CO_2 HnP had little effect on the ultimate oil recovery. However, due to changes in the conductivity of the entire core, significant differences in oil recovery were observed during the first two cycles (Li et al., 2019). In the single perforation stage, two fractures yield a higher oil recovery than the single fracture, as well as configurations with three or four fractures. This is attributed to the larger CO_2 invasion area associated with two fractures compared to other configurations. And the distance for CO_2 invasion along the fractures decreases with the increasing number of fractures, which might be resulted from the fracture interference (Yu et al., 2014). The fractured core experiments also confirmed that more fractures do not necessarily lead to higher oil recovery. Core permeability and the process of creating fractures are likely to be important factors affecting recovery (Yu et al., 2021). Fracture connectivity is also a critical factor affecting reservoir development after hydraulic fracturing. Numerical simulation studies have shown that good fracture connectivity leads to enhanced fracture conductivity, which in turn improves the oil recovery factor and CO_2 utilization efficiency during CO_2 HnP (Wei et al., 2021; Zhao et al., 2018). In addition, the mechanical properties of the rock also have a significant impact on the conductivity of hydraulic fractures. Laboratory experiments have shown that higher Young's modulus and lower Poisson's ratio indicate greater rock brittleness, which enhances fracture conductivity and thus improves the oil recovery (Xie et al., 2020). However, there is limited research on CO_2 HnP laboratory experiments under the conditions of hydraulic fractures (propped and unpropped). In this paper, we highlight the importance of fractures in CO_2 HnP for low-permeability heavy oil reservoirs with propped and unpropped fractures under different confining pressures. A relationship between the apparent permeability of the fractured cores and the fracture apertures is derived. The production dynamic from the core samples is monitored using nuclear magnetic resonance (NMR) to enable the derivation of such a relationship. This research is essential to the understanding of CO_2 HnP production in fractured low-permeability heavy oil reservoirs. Additionally, the effects of other factors such as oil viscosity, temperature, and pressure on the CO_2 HnP oil recovery factor in fractured cores are also investigated.

2. Experimental methods

2.1. Materials

The oil samples were prepared from dehydrated degassed crude oil of a low-permeability heavy oil reservoir block in the Xinjiang Oilfield, mixed with kerosene. The oil sample has a density of 0.9126 g/cm^3 and a viscosity of 344.67 mPa·s at the formation temperature of 70 °C. The viscosity–temperature curve of the oil is shown in Fig. 1.

The core samples were low-permeability sandstones provided by Beijing Tiandi Kaiyuan Geological Technology Co., Ltd. (Beijing, China). The petrophysical properties of the cores were similar to those of the low-permeability heavy oil reservoirs in the Xinjiang Oilfield, as shown in Table 1. CO_2 (≥ 99.8% pure) was supplied by Qingdao Hengyuan Gas Co., Ltd. (Qingdao, China).

2.2. Experimental setup

The core holder used in the HnP experiments was manufactured by Jiangsu Haian Scientific Instrument Co., Ltd. (Jiangsu, China), with a maximum pressure resistance of 40 MPa and a maximum temperature resistance of 200 °C. An ISCO plunger pump (Model 100DX, Teledyne Co., Ltd., USA) was used to saturate the core with heavy oil and provide injection pressure during the injection stage of the HnP experiments. A schematic representation of the CO_2 HnP experimental setup is shown in Fig. 2.

The viscosity of crude oil at different temperatures was measured using an MCR-302 Anton Paar rheometer (Anton Paar, Austria). The core fracturing device, manufactured by Jiangsu Haian Scientific Instrument Co., Ltd. (Jiangsu, China), was used to create the different fractures. The fractures produced by this device were continuous along the axial direction of the core, with morphological characteristics similar to in-situ fractures in the formation. The core fracturing procedure is provided in the Supplementary Material. The VHX6000 3D microscope (frame rate 15–50 frames/s, Keyence, Japan) was used to observe the fracture morphology and measure the surface roughness in different areas of the fractures.

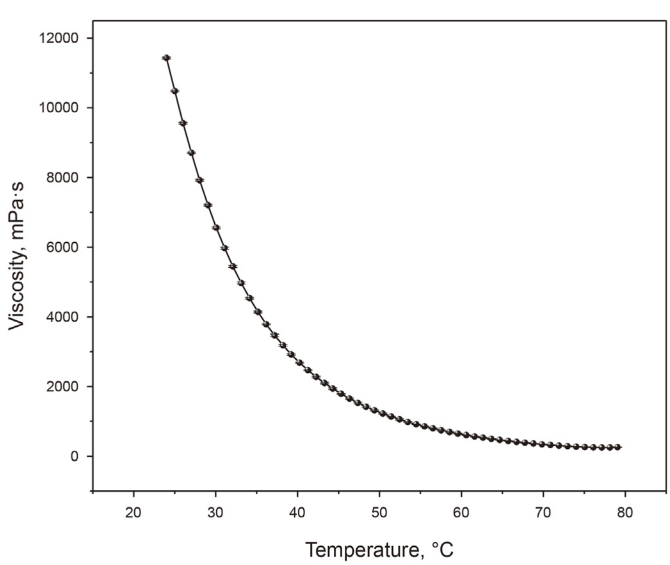

Fig. 1. Viscosity–temperature curve of the crude oil at a shear rate of 170 s^{-1}.

MesoMR23-060 NMR imaging system was used for core imaging (Suzhou Niumag Analytical Instrument Corporation, Suzhou, China). This equipment features an independent pulse control module and a radio frequency (RF) transmission and reception circuit, significantly improving the accuracy and stability of the pulse sequences and the signal-to-noise ratio of the NMR signals. It allows for precise characterization of fluid signals in pore sizes ranging from 2 nm to 1 mm. Mercury intrusion pore size analyzer, PoreMaster 60 (Anton Paar, Austria), was used for the mercury intrusion test, with a pore size measurement range of from 3.6 nm to 1100 μm.

2.3. Experimental procedures

The low-permeability cores used in the experiments were placed in an oven and dried at 105 °C for 12 h before being removed to measure the dry weight. Subsequently, cores were placed into a high-temperature and high-pressure intermediate container, and vacuum was applied for 24 h using a vacuum pump. Following vacuuming, heavy oil was injected into the intermediate container, where the plunger pump was set at constant pressure for 24 h after the pressure was increased to 20 MPa. No decrease in pressure was observed in the intermediate container, indicating that the cores were fully saturated with heavy oil. The oil saturated cores were then removed, the wet weight was measured, and the T_2 spectra were determined using NMR. Additionally, a core sample from the same block with identical permeability was selected for mercury intrusion test to convert T_2 into core pore sizes.

Before the NMR testing, the MesoMR23-060 NMR imaging system was preheated to ensure that the probe and magnet maintained a constant temperature. Once the system stabilized, the core sample was placed inside a glass tube and positioned in the sample chamber, ensuring that the center of the sample aligned with the center of the magnetic field. The CPMG sequence was selected, and the specific testing parameters were set as detailed in Table 2. The measurement was then initiated. The echo train signals collected with the CPMG sequence were inverted to obtain the T_2 spectrum.

The heavy oil saturated cores were fractured according to the experimental scheme shown in Table 1. The fractured cores were placed in the core holder, as shown in Fig. 2. The temperature was adjusted to 70 °C, corresponding to the reservoir temperature, and the initial pressure of the cores was set to 16 MPa. After aging the cores for 12 h, high-pressure CO_2 was continuously injected into the core holder from the injection end at a constant pressure of 16 MPa for 3 h, while simultaneously adjusting the confining pressure to 4 MPa higher than the core pressure. Following CO_2 injection, the injection valve was closed, and the decrease in water volume within the pump was recorded, representing the volume of CO_2 injected at 16 MPa. And the cores were soaked for 12 h. The density of CO_2 at 16 MPa and 70 °C can be obtained from the website of the National Institute of Standards and Technology (NIST), allowing the mass of the injected CO_2 to be determined. Then, the injection valve was opened, and the oil was produced at the same production rate controlled by the valve. The weight of the oil was measured real-time using a balance, and the oil production data as well as pressure data were recorded at different times. The experiment was stopped when the pressure decreased to 1.5 MPa, signaling the maximum oil recovery for a given cycle. Three cycles were run by repeating the above HnP steps. The cores were subjected to NMR analysis to determine the change in pore oil content after each HnP cycle. The cores were then replaced according to the experimental

Table 1
The parameters of the core samples.

Core No.	Length, mm	Diameter, cm	Permeability, mD	Saturated oil, mL	Fracture condition
#1	60.24	2.52	25.61	4.12	Fracture-free core
#2	60.32	2.50	24.86	4.21	Single fracture core
#3	60.28	2.48	24.24	4.30	Single fracture core with end surface sealed
#4	60.14	2.46	24.54	4.26	Propped fracture core
#5	60.18	2.54	25.10	4.21	Propped fracture core
#6	60.20	2.52	25.72	4.08	Unpropped fracture core
#7	60.22	2.50	25.80	4.23	Unpropped fracture core
#8	60.18	2.46	25.08	4.18	Propped fracture core
#9	60.10	2.50	26.08	4.15	Propped fracture core
#10	60.24	2.52	25.50	4.03	Unpropped fracture core
#11	60.14	2.50	25.43	4.23	Unpropped fracture core
#12	60.10	2.54	25.80	4.11	Propped fracture core
#13	60.22	2.52	25.41	4.02	Propped fracture core
#14	60.19	2.56	24.76	3.89	Propped fracture core
#15	60.26	2.52	25.16	4.32	Propped fracture core
#16	60.07	2.50	25.99	4.26	Propped fracture core
#17	60.16	2.50	24.89	4.18	Propped fracture core

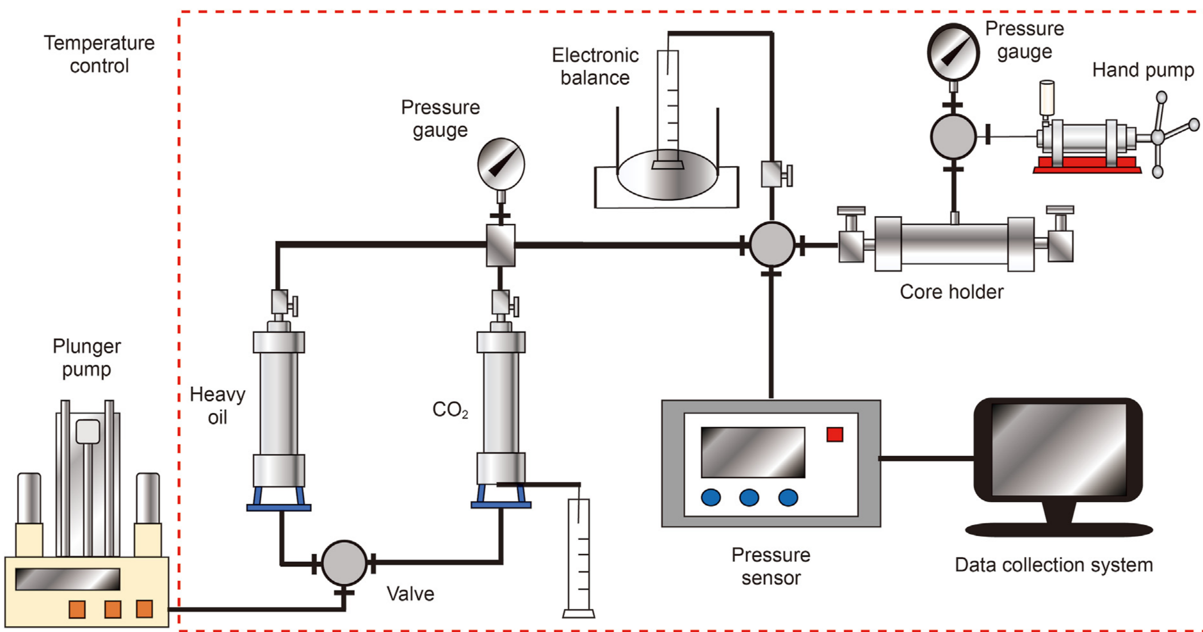

Fig. 2. Schematic diagram of the CO_2 HnP experimental setup.

Table 2
The parameters of CPMG sequence.

Parameter	Description	Value
SF, MHz	Spectrometer frequency	21
O1, Hz	Spectrometer frequency offset of the first channel	239824.5
P1, μs	The width of 90-degree RF pulse	19
P2, μs	The width of 180-degree RF pulse	37.04
TW, ms	The waiting time between two scans of sampling data	4000
RFD, ms	Time interval between 90-degree RF and the beginning of signal acquisition	0.08

scheme, and the HnP experiments were repeated to compare different fracture conditions.

3. Results and discussion

3.1. Effect of fracture conditions on CO_2 HnP

CO_2 HnP experiments were conducted on core samples with fracture-free, single fracture, and single fracture with end surface sealed. Fig. 3 shows the variations in oil recovery rate and oil recovery factor with production pressure during the CO_2 HnP process under different fracture conditions.

During the production stage, the rate of oil recovery increases followed by a decrease coinciding with the decreasing production pressure, for all the different runs. The production stage of CO_2 HnP in the fracture-free core can be divided into three stages. Initially,

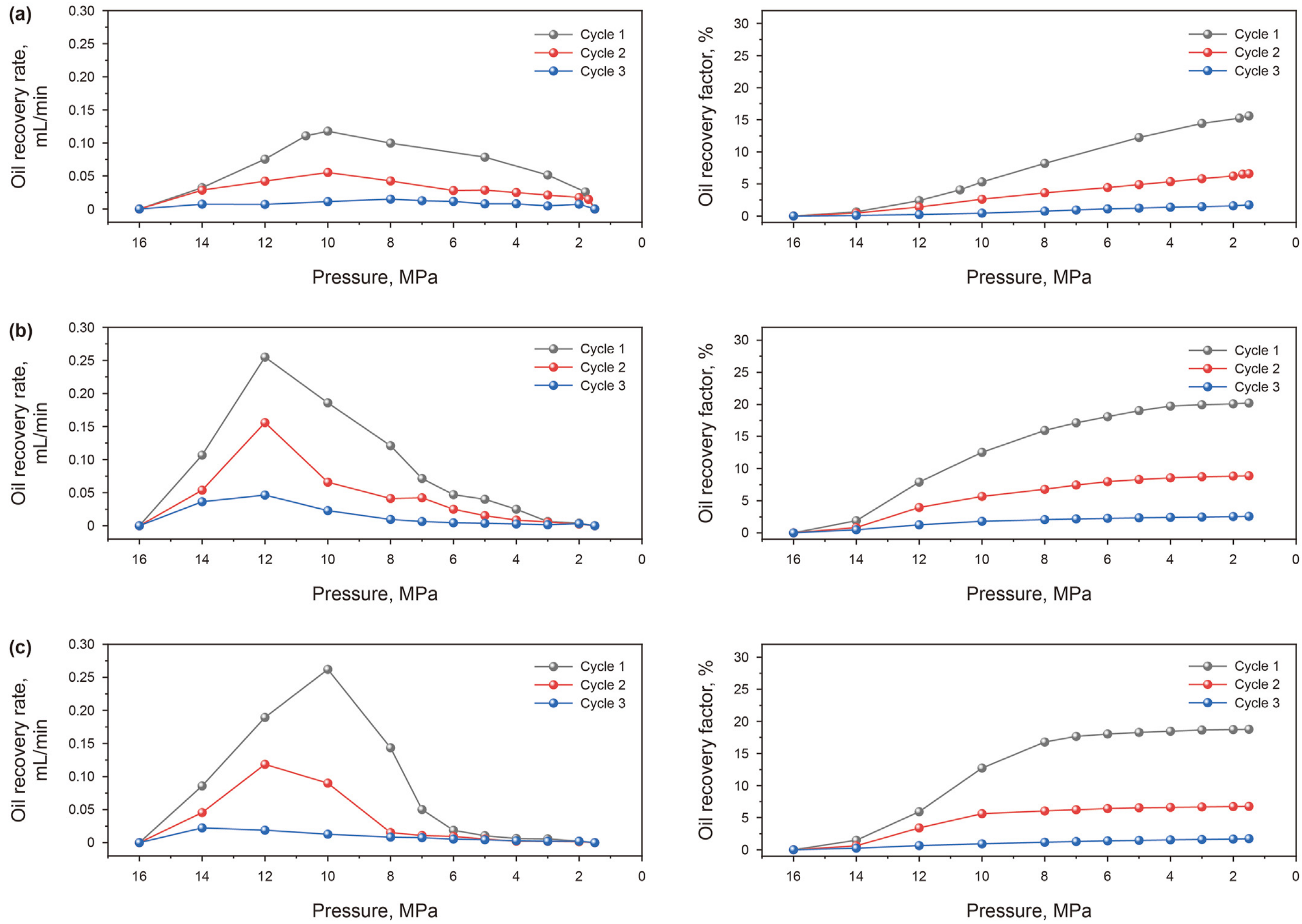

Fig. 3. Variations in oil recovery rate and oil recovery factor with production pressure for different fracture conditions: (**a**) fracture-free core, (**b**) single fracture core, and (**c**) single fracture core with end surface sealed.

during the early stage of production, the oil recovery rate is relatively low, resulting in a lower oil recovery factor. In the middle stage of the HnP production step, the oil recovery rate gradually increases with the decreasing pressure. The maximum oil recovery rate of 0.118 mL/min is achieved at 12 MPa during the first cycle, after which the oil recovery rate gradually decreases. In the later stage of the production step, the oil recovery rate remains relatively low and gradually decreases to zero. The injected CO_2 in the core is mainly in the form of free CO_2 and dissolved CO_2 in the heavy oil. In the early times of the HnP production stage, due to the high pressure inside the core, a small portion of heavy oil is carried out by free CO_2. At this point, due to the high viscosity of the heavy oil, the produced fluid is mainly free CO_2. The oil recovery factor is, therefore, low in the initial production stage. With the release of free CO_2, the pressure inside the core gradually decreases and the CO_2 originally dissolved during the soaking stage gradually separates. However, due to the high viscosity of the heavy oil, the separated CO_2 disperses within the heavy oil, giving rise to foamy oil, which increases the elastic energy of heavy oil and enhances the oil recovery rate and oil recovery factor. As the pressure decreases further, the oil recovery rate gradually decreases. When the pressure inside the core drops to 1.5 MPa, the subsequent HnP cycle begins.

The presence of fracture within the core significantly increases the oil recovery rate during the early and middle HnP stages of the production step. In the first HnP cycle for the single fracture core, the oil recovery rate peaks at 0.255 mL/min when the injection pressure decreases to 12 MPa, far higher than that of the fracture-free core. The maximum oil recovery rate of the single fracture core with end surface sealed is higher, 0.262 mL/min, however its duration is short. The oil recovery rate declines rapidly after reaching this peak. During the early stage of production, heavy oil surrounding the fracture is rapidly produced, leading to a rapid decrease in core pressure. This causes the oil recovery rate to reach its peak early, with the maximum oil recovery rate slightly exceeding that of the single fracture core. However, due to the sealed end surface, once the easily recoverable oil surrounding the fracture is depleted, the oil located farther from the fracture or near the core's end surface can only be produced through the fracture. This significantly increases flow resistance, resulting in a sharp decline in the oil recovery rate after the peak. In the fractured cores, the fractures increase the contact area between CO_2 and heavy oil, allowing more CO_2 to directly interact with the oil, hence reducing the viscosity of the heavy oil. During the injection stage of CO_2 HnP, under the effect of the pressure differential, CO_2 displaces the crude oil from the macropores around the fracture into the fracture through Darcy's flow, while simultaneously transmitting pressure deeper into the fracture and the adjacent matrix. Additionally, during the soaking stage of the CO_2 HnP process, CO_2 gradually dissolves into the crude oil in contact and diffuses into the crude oil within the deeper pores of the matrix. Therefore, during the production step, the heavy oil containing dissolved CO_2 in larger pores quickly flows into the fracture. In the meantime, the distance and flow resistance toward the fluid in the smaller pores as it flows through the larger pores into the fracture are significantly reduced. Consequently, the oil recovery rate substantially increases in the early and middle stages of the production step. Additionally, the CO_2 HnP oil recovery factor of the single fracture core with the end surface sealed is also higher than that of the fracture-free core. This indicates that during the injection stage, CO_2 entering the matrix through the fracture is more effective than entering through the end surface of the core, further emphasizing the importance of fractures in the CO_2 HnP process. In fracture-free cores, the heavy oil can only flow through pores and throats. As the distance from the production end increases, the flow resistance to heavy oil also increases significantly. Subsequently, the heavy oil is unable to reach the production end leading to noticeably lower oil recovery factor compared with the fractured cores.

By conducting NMR analysis on the cores before and after the HnP runs, the variation in hydrogen signal within the cores under different relaxation times can be obtained. Coupling the NMR analysis with the pore radius distribution results obtained from mercury intrusion experiments enables converting the relaxation time on x-axis into pore radius. The specific conversion process and the conversion coefficient calculation are provided in the Supplementary Material. Additionally, the ratio of the hydrogen signal in specific size pores to the total hydrogen signal of the saturated oil core is taken as the oil saturation in the specific size pores. Accordingly, the distribution of oil saturation in pores of different sizes is determined. The characteristics of the T_2 curves from NMR analysis of the saturated oil core samples suggest good connectivity between the pores of the low-permeability core in the experiments (Zhang et al., 2021b). The heavy oil is primarily distributed within pores with radii ranging from 0.02 to 20 μm. The literature describing pore sizes in low-permeability and tight oil reservoirs is inconsistent in the classification standards (King et al., 2015). In this study, we rely on the pore classification system recommended by Qian et al. (2020), as the physical properties of their core samples are similar to those used in our experiments. Based on

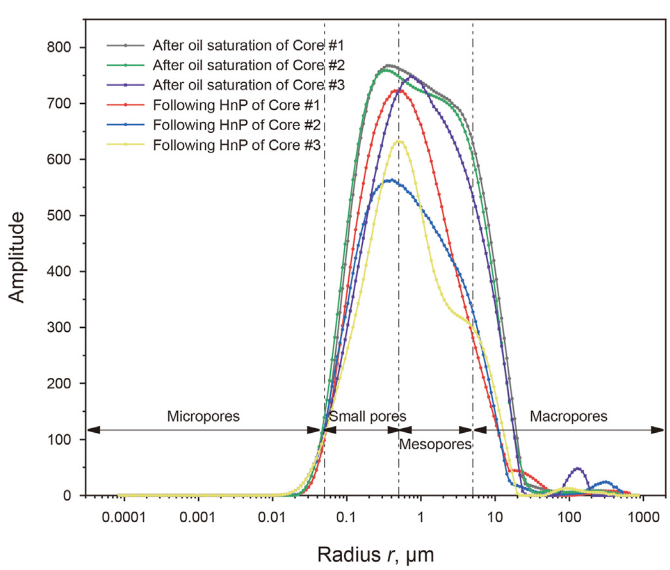

Fig. 4. NMR results of low-permeability cores with CO_2 HnP under different fracture conditions.

the pore radius, pores can be classified into four types: micropores (radii < 0.05 μm), small pores (radii from 0.05 to 0.5 μm), mesopores (radii from 0.5 to 5 μm), and macropores (radii > 5 μm).

The NMR results for low-permeability cores under different fracture conditions are shown in Fig. 4. Fig. 4 suggests that the heavy oil primarily resides within the small pores, mesopores, and macropores of the saturated core. Following the first HnP cycle in the fracture-free core, a significant decrease in signal amplitude in the mesopores and macropores is observed. The amplitude in the small pores suffered minimum decrease, whereas the amplitude in the micropores did not change. Under fracture-free condition, heavy oil is primarily produced from the mesopores and macropores. For the single fracture core, the small pores and mesopores exhibit more pronounced decrease in heavy oil saturation compared with the fracture-free core. The presence of a fracture increases the sweep area of CO_2, allowing it to diffuse into the mesopores and the small pores at the distal end of the core, hence significantly enhancing oil recovery. Additionally, the NMR signal curve of the single fracture core shows a slight left shift following HnP indicating that the injected CO_2 reached and mobilized the oil in the smaller pores of the core. As shown in Fig. 4, the single fracture core with end surface sealed still achieves considerable oil recovery factor, and the heavy oil from the mesopores and macropores of the core is primarily produced. Unlike the fracture-free core, the majority of the heavy oil recovered is from the mesopores and the macropores surrounding the fracture of the single core with end surface sealed. In the injection step, CO_2 can displace the crude oil in the large pores around the fracture under the effect of differential pressure, and during the soaking step, CO_2 within the macropores can gradually diffuse into nearby mesopores. Consequently, during the production stage, the heavy oil with the dissolved CO_2 in both macropores and mesopores can be produced through the fracture. In contrast, in the fracture-free core, the heavy oil primarily comes from the mesopores and macropores near the injection end of the core, mainly due to the difference in the sweep area of CO_2. In addition, the presence of the fracture significantly reduces the residual oil saturation in small pores and mesopores. This indicates that the fracture allows CO_2 to effectively diffuse into these smaller pores and mesopores, enhancing oil recovery during the production stage. Moreover, these small pores and mesopores can serve as storage space for the injected CO_2, allowing CO_2 to diffuse into further regions of the core in subsequent cycles. This process improves the oil recovery degree of small pores and mesopores over multiple HnP cycles.

Based on NMR results, the extent of oil recovery from various pores in low-permeability cores under different fracture conditions is calculated and presented in Fig. 5. The highest extent of oil recovery occurs in the macropores of the three cores. The extent of oil recovery from micropores, small pores, and mesopores is greater in the fractured cores. Notably, the increase in the extent of oil recovery from small pores is the most significant, from 12.52% to 26.82%. In presence of a fracture, the sweep range of CO_2 increases. Once CO_2 enters the macropores surrounding the fracture, it can mobilize more oil from the connected mesopores and small pores through diffusion and extraction. Due to the extensive sweep area of CO_2, combined with the high viscosity and poor flowability of the oil, the heavy oil produced from small pores at the distal end of the core may remain in the macropores surrounding the fracture. Thus, a slight decrease in the extend of oil recovery from the macropores of the single fracture core occurs.

Oil recovery factor and gas consumption ratio under different fracture conditions are shown in Fig. 6. Eq. (1) presents the gas consumption ratio (Li et al., 2022).

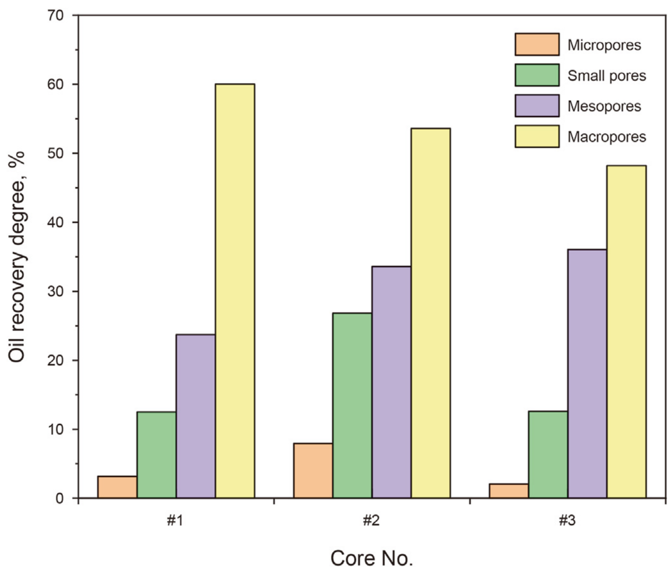

Fig. 5. Oil recovery degree in different size pores of low-permeability cores during CO_2 HnP experiments under different fracture conditions.

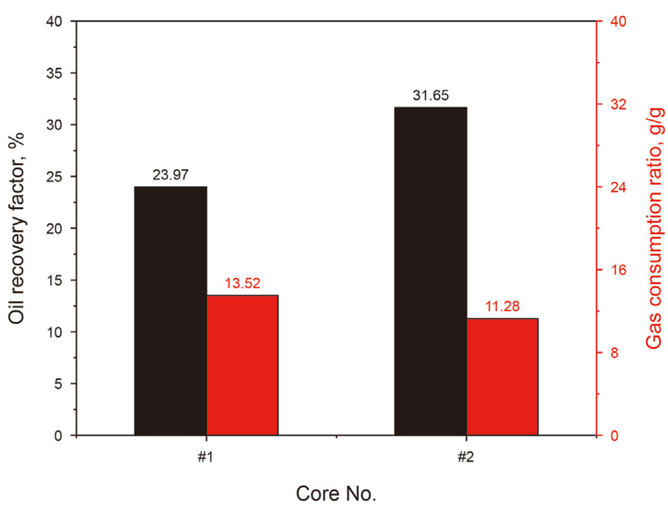

Fig. 6. Oil recovery factor and gas consumption ratio of CO_2 HnP in low-permeability cores under different fracture conditions.

$$N=\frac{m_g}{m_o} \tag{1}$$

where N is the gas consumption ratio, g/g; m_g is the mass of the injected gas, g; m_o is the mass of the produced oil, g.

Fig. 6 indicates that the presence of fracture not only enhances the oil recovery factor but also reduces the CO_2 gas consumption ratio, with the average gas consumption ratio over three cycles decreasing from 13.52 to 11.28 g/g. Although the fracture can serve as a storage site for the gas, the enhanced oil recovery compensates for the CO_2 consumption, rendering CO_2 HnP technique more economical. In addition, for more cost-effective application of CO_2 HnP technology, it is recommended to target reservoirs that are in close proximity to CO_2 sources, reducing transportation costs and improving economic efficiency. Therefore, in the actual development of low-permeability or tight reservoirs, combining hydraulic fracturing with CO_2 HnP can further optimize the production process. After hydraulic fracturing and spontaneous imbibition, CO_2 HnP not only replenishes reservoir energy but also takes advantage of the fractures generated during fracturing. The presence of these fractures significantly increases the contact area between CO_2 and oil, thereby enhancing oil recovery. Additionally, the fractures facilitate the injection of CO_2 into the depths of the reservoir, helping to mobilize trapped oil that would otherwise be inaccessible. The combination of fracturing and CO_2 injection makes oil production more economical, as it not only improves oil recovery but also reduces CO_2 gas consumption. By leveraging the combined benefits of fracture creation and CO_2 injection, operators can achieve more sustainable and cost-effective oilfield development.

3.2. Effect of propped and unpropped fracture

The above experimental results demonstrate that the presence of fracture can significantly enhance the oil recovery factor of heavy oil from low-permeability cores. However, in actual hydraulic fracturing processes, influenced by factors such as geostress, rock strength, and natural fractures, a variety of complex fracture networks form. Primary fractures are propped by proppants, whereas secondary fractures are unpropped and are created by shear slippage. Both primary and secondary fractures possess certain conductivity under the effect of the closing stress. However, the conductivity of unpropped fractures decreases gradually with pressurization time, and the rate of decrease slows over time. This work systematically investigates the impact of propped and unpropped fractures on the effectiveness of CO_2 HnP, as shown in Fig. 7.

Oil recovery factor for each cycle of the HnP in 20-mesh proppant propped fracture core (Core #4), 40-mesh proppant propped fracture core (Core #5), 1.5-mm slippage unpropped fracture core (Core #6), and 3.0-mm slippage unpropped fracture core (Core #7) are shown in Fig. 8. And the sand concentration for all propped fracture cores was kept constant at 1.5 kg/m^2. The oil recovery factor in propped fracture cores is significantly higher than in unpropped fracture cores, while both are higher than in a single fracture core. The 20-mesh proppant propped fracture core achieved the highest oil recovery factor of 38.44%, representing an increase of 6.79% compared to the single fracture core. Accordingly, for the same proppant fraction, the 20-mesh proppants provide better support than the 40-mesh proppants. The pores between the proppants are larger for fractures propped by larger-size proppants, thus enhancing the conductivity of the fracture. Proppant-filled fracture can take full advantage of the fracture, maintaining a higher fracture aperture under higher confining pressures. The fractures serve as storage sites for CO_2, allowing more CO_2 to be injected into the core. More CO_2 maintains the pressure within the core while enhancing the interaction with the heavy oil, hence increasing the oil recovery factor. The oil recovery factor of the 1.5-mm slippage unpropped fracture core is only slightly higher, 0.80%, than that of the 3.0-mm slippage unpropped fracture core. The conductivity of the fracture produced by shear misalignment primarily depends on the roughness of the fracture surfaces following the application of the closing pressure (Ghanizadeh et al., 2016; Sharma and Manchanda, 2015; Wang and Sharma, 2018). Under the confining pressure of 20 MPa, the roughness of the fracture in the two unpropped experimental cores is not significantly different, hence the oil recovery factor shows only minor variations.

NMR test results of HnP for the 20-mesh proppant propped fracture core and the 1.5-mm slippage unpropped fracture core are shown in Fig. 9. Heavy oil from small pores and mesopores in the 20-mesh proppant propped fracture core is significantly greater than that in the unpropped fracture core, while the difference in oil recovery from the micropores and the macropores are minimal. Under the confining pressure of 20 MPa, the aperture of the

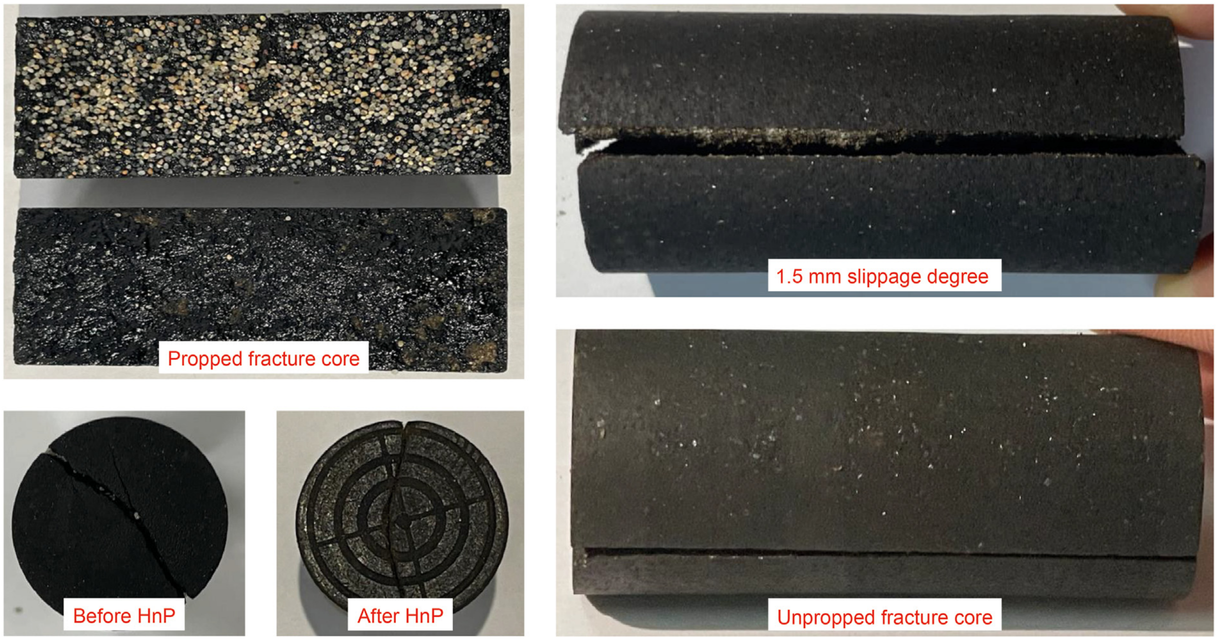

Fig. 7. Experimental cores with propped fractures and unpropped fractures.

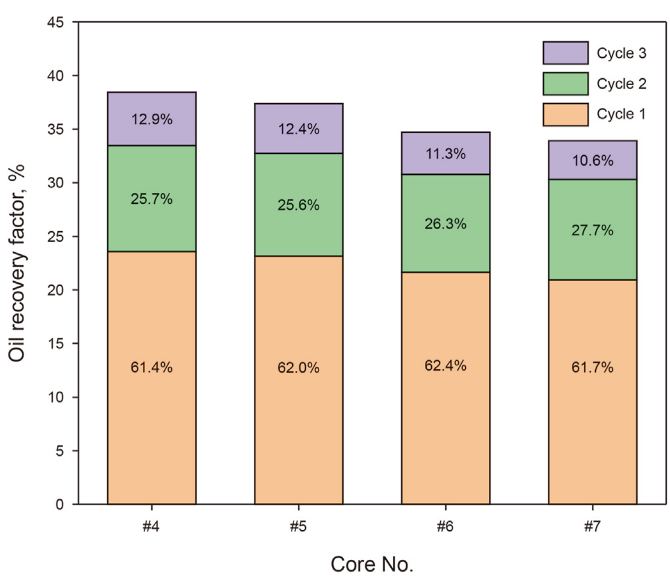

Fig. 8. Oil recovery factor of CO_2 HnP from propped and unpropped cores.

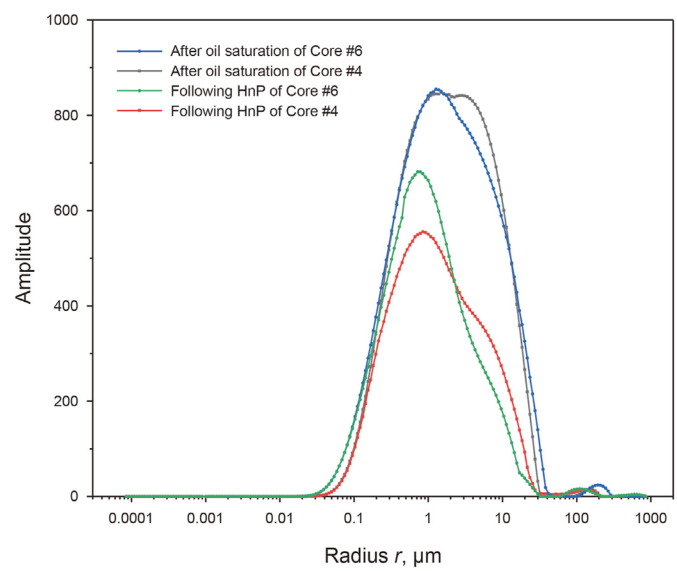

Fig. 9. NMR test results of CO_2 HnP for the 20-mesh proppant propped fracture core (Core #4) and the 1.5-mm slippage unpropped fracture core (Core #6).

propped fracture is greater than that of unpropped fracture, allowing more CO_2 to enter the macropores of the core along the fracture during the injection stage of CO_2 HnP. The fracture also works as a storage site, holding more CO_2. During the soaking step, CO_2 diffuses into more of the small pores and mesopores, resulting in a higher oil recovery from these pores. Additionally, compared to the saturated oil NMR curve, the NMR curve for the 20-mesh proppant propped fracture starts to decrease at a smaller pore size, indicating that the lower limit of pore sizes accessible by CO_2 in the core has decreased, allowing the oil recovery of heavy oil from smaller pores.

For the actual fracturing processes, both propped and unpropped fractures may close under high geostresses, hence reducing the conductivity and greatly affecting the oil recovery factor. Therefore, it is essential to conduct HnP experiments on fractured cores under different confining pressures. In this study, varying confining pressures (20, 30, 40 MPa) are used to simulate the closure pressures, with Core #8 and Core #9 for the propped fracture and Core #10 and Core #11 for the unpropped fracture.

Oil recovery factor in low-permeability cores under different confining pressures are illustrated in Fig. 10. Fig. 10 suggests that with increasing confining pressure, the oil recovery factor significantly decreases. While the permeability of the fracture decreases, the matrix pore throats are also compressed. Under the influence of the stress, rock particles are compressed, undergo relative displacement, and rearrange, leading to reduced average pore radius and average throat radius. Consequently, the matrix permeability decreases and the oil recovery factor declines (Guo

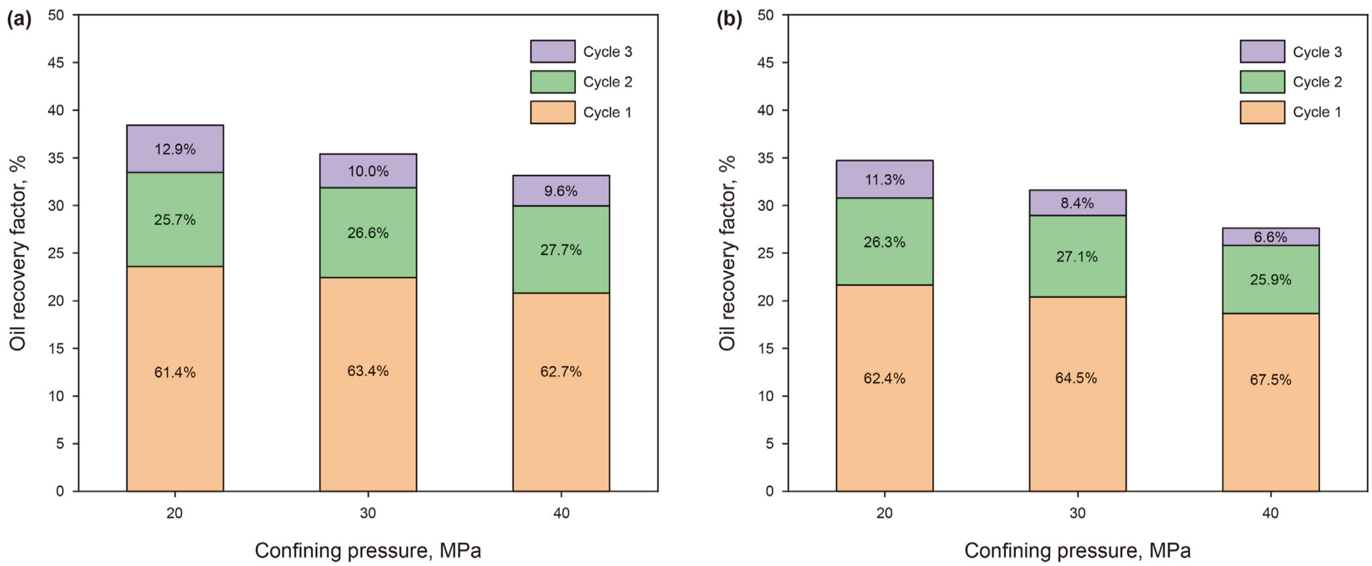

Fig. 10. Oil recovery factor of CO_2 HnP in low-permeability cores under different confining pressures: (**a**) 20-mesh proppant propped fracture core and (**b**) unpropped fracture core.

et al., 2013; Wang and Sharma, 2018; Zhou et al., 2019a). The reduction in the oil recovery factor is more pronounced in unpropped fracture cores with increasing confining pressure. When the confining pressure rises from 20 to 40 MPa, the oil recovery factor decreases by 7.11%. In presence of proppants, the fractures cannot be completely closed under the influence of the confining pressure and can still maintain a significant aperture. Unlike propped fractures, unpropped fractures primarily rely on point contacts and have strong stress sensitivity. As the closure pressure increases, many micro-protrusions on the fracture surfaces are crushed, causing the fracture to almost completely close at some locations (Wang et al., 2020), as schematically shown in Fig. 11. The most noticeable reduction in the oil recovery factor in unpropped fracture cores occurs in the third cycle, which is also due to the significantly reduced fracture aperture caused by prolonged exposure to high closure pressures. Propped fractures play a crucial role in maintaining open flow channels over an extended period of time by using proppants. These fractures allow for lower flow resistance, enabling CO_2 or other injection agents to more efficiently penetrate the reservoir, thereby enhancing oil recovery. The sustained openness of propped fractures ensures crude oil flows more freely, even under higher confining pressures. In contrast, unpropped fractures tend to gradually close during production as the reservoir pressure changes. While they can provide effective flow channels during the early stage of production, the closure of these fractures increases flow resistance, which can lead to a decrease in oil recovery over time. However, unpropped fractures can still be beneficial in the short term, particularly in lower pressure conditions.

To quantitatively assess the impact of confining pressure on unpropped fractures, the method proposed by Zheng (2023) has been optimized for calculating fracture aperture and permeability

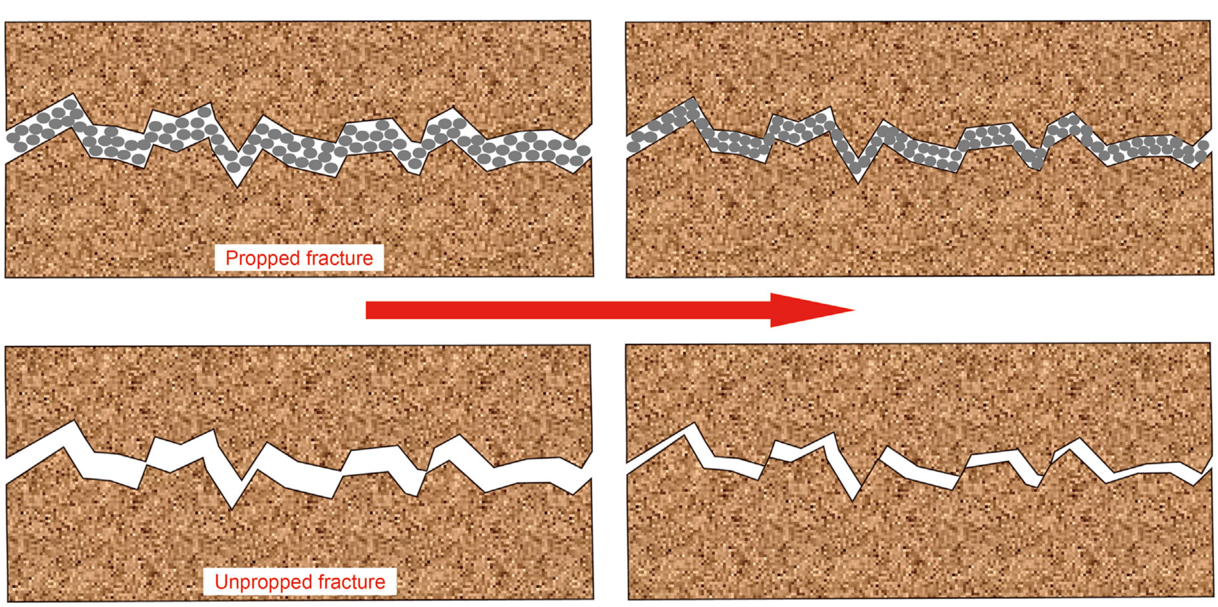

Fig. 11. Process of propped and unpropped fractures closure under stress.

under different confining pressures. The local cubic law (LCL) is commonly used to describe fluid flow in a single fracture, simplifying the fluid as incompressible. Treating the fracture as an ideal smooth parallel plate, using Navier–Stokes equation leads to a distribution of flow velocities across the fracture under ideal conditions. However, actual fractures often have pronounced roughness. To obtain a more realistic depiction of fluid flow in rock fractures, the LCL has been refined (Charlez, 1997; Kolditz, 2001; Snow, 1969). Ignoring the tortuosity of the fractures, Zhang et al. (2019) modified the LCL to

$$q_{\mathrm{f}}=\frac{dw^3}{12\mu L}\Delta P\frac{1}{1+0.61308\left(\frac{S_{\mathrm{a}}}{w}\right)^{0.60912}} \tag{2}$$

where q_{f} is the volumetric flow rate in the fracture, μm^3/s; d is the fracture width, μm; w is the fracture aperture, μm; L is the fracture length, μm; μ is the viscosity of the fluid, Pa·s; ΔP is the pressure drop, Pa; S_{a} is the absolute surface roughness, μm. Based on the revised equation, and incorporating Darcy's law along with the flow regime of injected fluids in fractured core systems proposed by Dong et al. (2018), Eq. (3) describes the apparent permeability of the fractured core and the fracture aperture. The detailed derivation of Eq. (3) is given in the Supplementary Material.

$$\overline{k}=\frac{\pi k_{\mathrm{m}}D\Big/4+w^3\Big/\left[12+7.35696(S_{\mathrm{a}}/w)^{0.60912}\right]}{\pi D/4+w} \tag{3}$$

where $\overline{k}$ is the average permeability of the fractured core (apparent permeability), μm^2; k_{m} is the permeability of core matrix, μm^2; D is the diameter of the core, μm. The surface roughness in the equation can be measured using a VHX6000 3D microscope. A commonly reported method in the literature for calculating fracture aperture is the thin-slice area method (Li et al., 2020b), as shown in the following equation:

$$k_{\mathrm{f}}=\frac{cw^3L}{S} \tag{4}$$

where k_{f} is the permeability of the fractured core, 10^{-3} μm^2; w is the fracture aperture, μm; L is the length of the fracture, cm; S is the thin-slice area, cm^2; c is a constant fracture coefficient, which is related to the distribution of the fracture in the thin slice. This method assumes that the fracture walls are smooth thin slices, which leads to significant errors in the calculated fracture aperture. Based on the modified local cubic law, the relative roughness of the fracture walls is taken into account, and a more accurate equation for calculating the fracture aperture is derived, as shown in Eq. (3).

Permeability tests under different confining pressures were conducted on an unsaturated oil unpropped fracture core and a fracture-free core, as shown in Fig. 12. Fig. 12 reveals that at the confining pressure of 10 MPa, the measured permeability of the unpropped fracture core is 60.93 mD, significantly higher than that of the fracture-free core. As the confining pressure increases, the permeability of both the fracture-free and unpropped fracture cores markedly decreases, with the rate of decrease gradually leveling off as the confining pressure rises.

Based on the measured matrix permeability and the apparent permeability of the unpropped fracture core under different confining pressure conditions, combined with the fracture surface roughness data obtained from microscope tests, the fracture aperture of unpropped fracture core under different confining pressures can be calculated using Eq. (3), as shown in Fig. 13. With increasing confining pressure, the fracture aperture of unpropped fracture

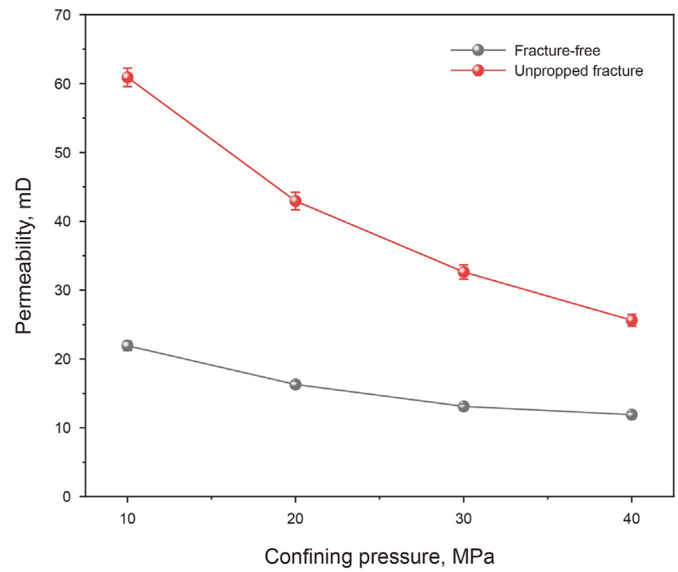

Fig. 12. Variation of core apparent permeability under different confining pressures.

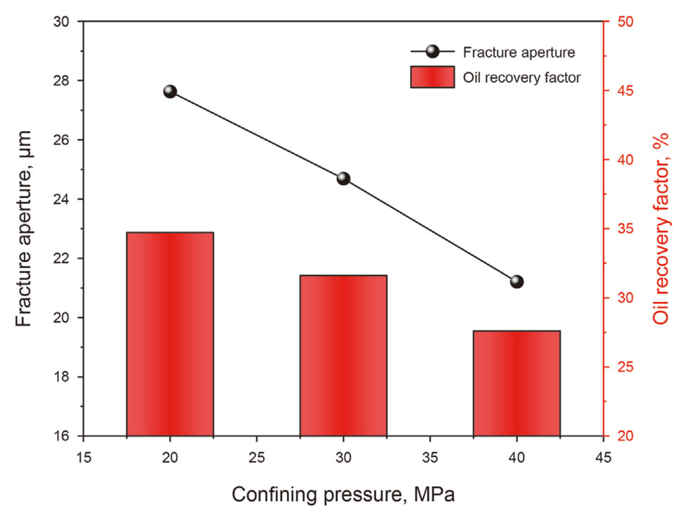

Fig. 13. Variations of core fracture aperture and oil recovery factor under different confining pressures.

core significantly decreases. When the confining pressure is 20 MPa, the fracture aperture is 27.63 μm, which reduces to 21.21 μm when the confining pressure is increased to 40 MPa. The increase in confining pressure significantly affects fracture aperture and fracture conductivity. For propped fractures, proppants with higher hardness can maintain a considerable fracture aperture even under higher confining pressures, resulting in only a slight reduction in oil recovery during CO_2 HnP. However, the impact of increased confining pressure on unpropped fractures is more pronounced due to their strong stress sensitivity. Under high confining pressures, the micro-protrusions on the surface of unpropped fracture are crushed, reducing the roughness of the fracture surface and causing closure at certain locations. This leads to a substantial reduction in both fracture aperture and fracture conductivity. The reduction in fracture aperture decreases the available storage space for CO_2 and limits the amount of CO_2 injected during the injection stage. Moreover, the partial closure of unpropped fractures restricts the diffusion of CO_2 into the deeper regions of the matrix during the soaking stage, limiting CO_2 penetration to only the areas immediately surrounding the fracture. As a result, the mobilization of oil in the matrix farther from the fracture is less effective. Simultaneously, the decrease in fracture aperture and conductivity, combined with the altered CO_2 distribution, significantly impacts the oil recovery factor. As the fracture aperture decreases, the oil recovery factor also declines. Therefore, quantitatively characterizing fracture properties is crucial for CO_2 HnP production in fractured cores. Moreover, the research results may provide potential references for practical oilfield production. For instance, in the design of refracturing techniques, more emphasis could be placed on unpropped fracture sections, or CO_2 injection pressures could be appropriately increased to keep unpropped fractures open for extended periods.

3.3. Effect of other factors on CO_2 HnP performance in fractured cores

For low-permeability heavy oil reservoirs, the viscosity of the crude oil determines the choice of development method, making oil viscosity one of the critical factors to consider when applying CO_2 HnP in the presence of fractures. Based on this, CO_2 HnP experiments were conducted on 20-mesh propped fractured cores with oil samples of different viscosities. The viscosity–temperature curve for different oil samples is shown in Fig. 14. Among them, Oil sample #1 is the same oil sample used in previous experiments, with a viscosity of approximately 344.67 mPa·s at 70 °C. The viscosities of Oil sample #2 and Oil sample #3 at 70 °C are about 506.6 and 681.8 mPa·s, respectively.

The oil recovery factors of CO_2 HnP experiments on propped fractured cores with different oil samples are shown in Fig. 15. As can be seen from the figure, the oil recovery factor decreases significantly as the oil viscosity increases. When using Oil sample #3, the oil recovery factor decreases to 21.17%, even slightly lower than the oil recovery factor for CO_2 HnP in the fracture-free core. The increase in viscosity greatly reduces the mobility of the crude oil and increases flow resistance, with some heavy oil still remaining in the fracture after HnP, unable to be carried to the production end by CO_2. Although high-viscosity oil experiences a greater viscosity reduction after CO_2 injection, the viscosity is still higher than that of conventional oil at the same temperature, resulting in continued high flow resistance. Additionally, higher-viscosity crude oil tends to have higher asphaltene content, which can precipitate in the reservoir pores after multiple cycles of HnP, contributing to the very low oil recovery factor in the third cycle. The increase in heavy oil viscosity also impedes CO_2 diffusion during the soaking stage, resulting in a lower diffusion coefficient, which limits CO_2 mass transfer into the matrix farther from the fracture. This is another reason for the decline in CO_2 HnP oil recovery factor as oil viscosity increases.

Temperature is an inherent property of the reservoir and one of the uncontrollable factors influencing heavy oil recovery. Studying the effect of temperature on HnP oil recovery is of great significance for selecting CO_2 pilot test areas and predicting the CO_2 HnP performance. CO_2 HnP experiments were conducted on 20-mesh propped fractured cores at different temperatures (55, 70, 85 °C), and the oil recovery factors are shown in Fig. 16. As the

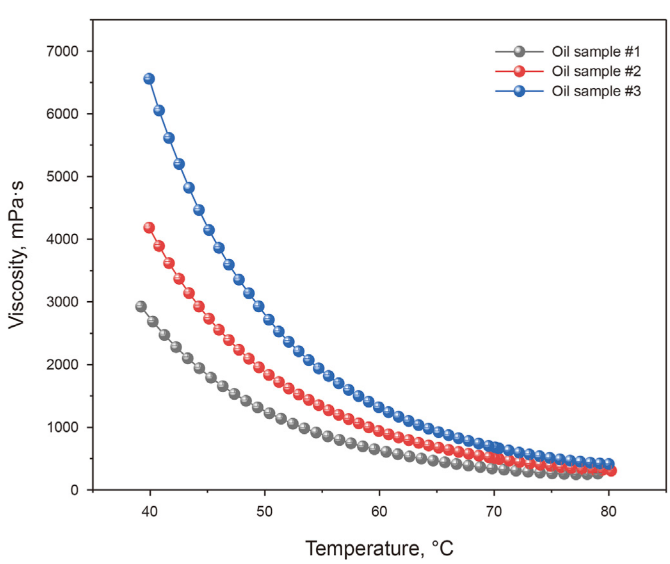

Fig. 14. Viscosity–temperature curves for different oil samples.

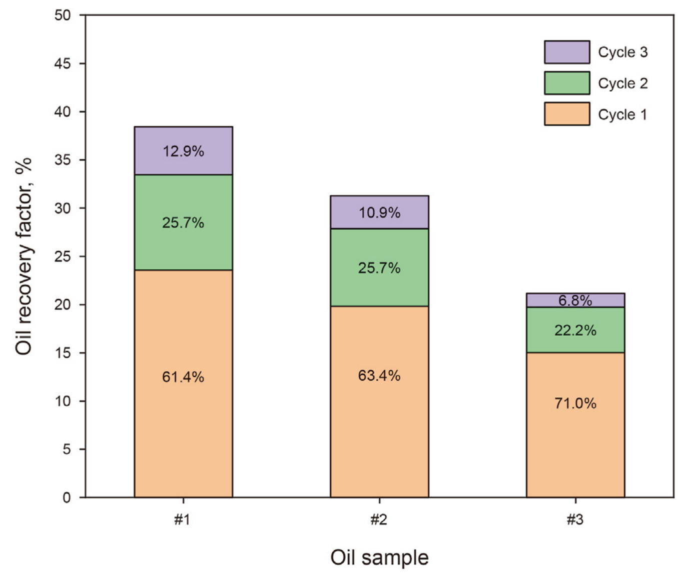

Fig. 15. Oil recovery factor of CO_2 HnP in propped fractured cores with different oil samples.

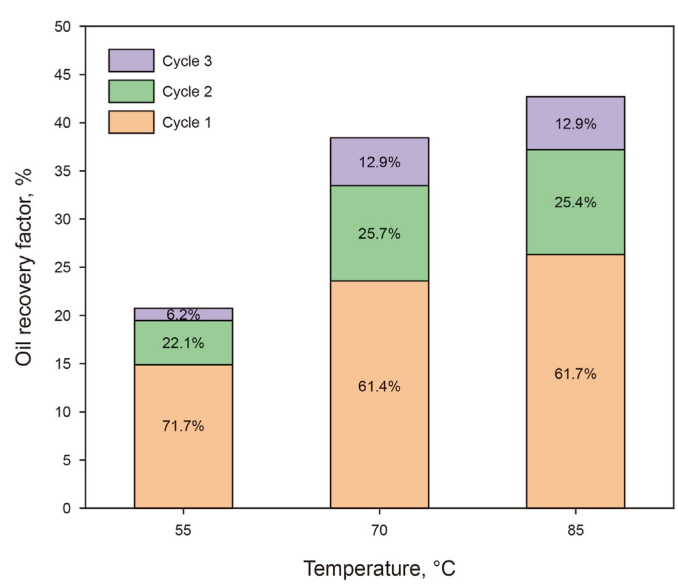

Fig. 16. Oil recovery factor of CO_2 HnP in propped fractured cores at different temperatures.

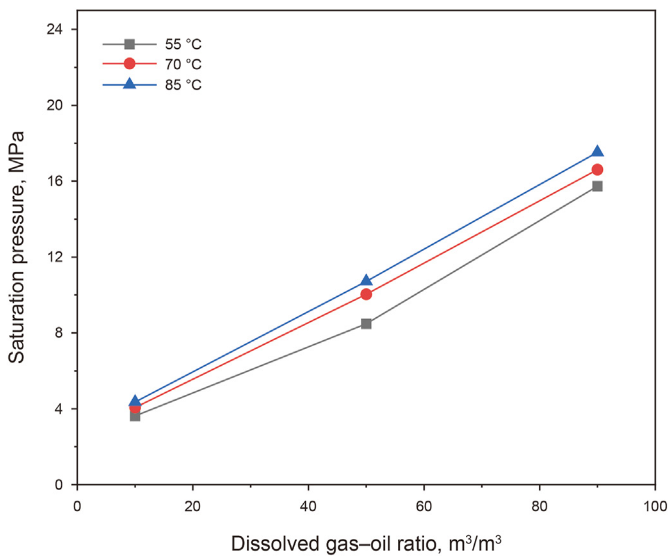

Fig. 17. Relationship between dissolved gas–oil ratio and saturation pressure at different temperatures.

experimental temperature increases, the oil recovery factor increases as well. This is primarily due to the significant reduction in heavy oil viscosity with higher temperatures. The most substantial decrease in oil viscosity occurs when the temperature rises from 55 to 70 °C, resulting in the largest increase in oil recovery. On one hand, the increase in temperature reduces crude oil viscosity and enhances the diffusion effect, which is beneficial for improving oil recovery. On the other hand, it decreases the solubility of CO_2 in heavy oil, as shown in Fig. 17. At the same saturation pressure, lower temperatures result in a higher dissolved gas–oil ratio, while rising temperatures accelerate the movement of CO_2 molecules, increasing the distance between them and ultimately reducing the CO_2 content dissolved in the heavy oil. However, under the conditions of this study, the reduction in crude oil viscosity with increasing temperature, which improves the heavy oil mobility, is clearly the dominant factor.

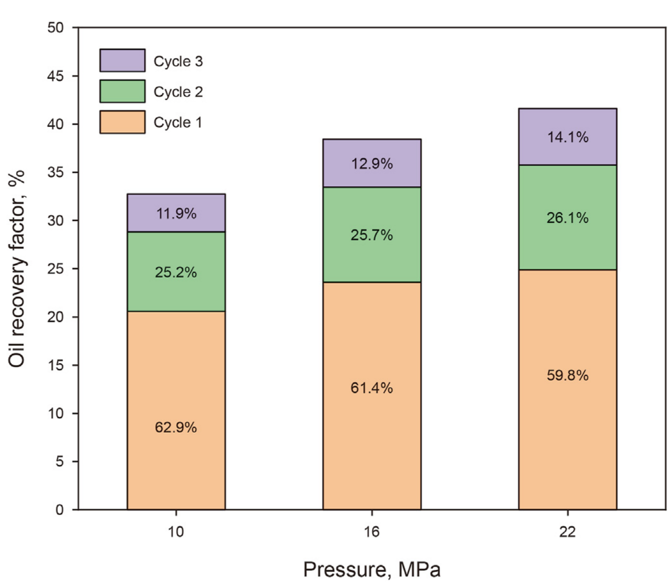

Fig. 18. Oil recovery factor of CO_2 HnP in propped fractured cores at different injection pressures.

The oil recovery factors of CO_2 HnP in propped fractured cores with different injection pressures are shown in Fig. 18. As the injection pressure increases, the oil recovery factor also increases. When the CO_2 injection pressure reaches 22 MPa, the recovery factor reaches 41.61%. Higher injection pressure allows more CO_2 to be injected during the injection stage of the HnP process, increasing the diffusion coefficient of CO_2 and enhancing the diffusion effect during the soaking stage. This results in more CO_2 diffusing into the matrix farther from the fracture. Additionally, injecting CO_2 at high pressure helps maintain fracture openness, an effect that may be more pronounced in unpropped fractured cores. In actual oilfield production, increasing the injection pressure during CO_2 HnP operations can also induce the extension of natural fractures in the reservoir, increasing the contact area between CO_2 and the crude oil in the matrix, reducing flow resistance for oil moving from the matrix to the production end, and thereby improving the oil recovery.

4. Conclusions

The role of propped and unpropped fractures on CO_2 huff-n-puff is elucidated through NMR production dynamic analysis of single fracture and fracture-free cores. A relationship between the apparent permeability of the fractured core and the fracture aperture is derived. This relation provides a quantitative description of the impact of fracture properties on CO_2 huff-n-puff method. The following conclusions can be drawn from this study:

(1) The presence of the fracture in the core significantly enhances both the oil recovery and the oil recovery rate during the early and middle stages of the CO_2 huff-n-puff production step. The cumulative oil recovery is increased by 7.68% compared to the fracture-free core. Fractures increase the contact area between CO_2 and heavy oil, hence promote gas dissolution and improve oil flowability. Additionally, CO_2 can rapidly fill the fracture during the injection stage and transmit pressure to the matrix, facilitating the rapid CO_2 diffusion during the soaking stage. Subsequently, fractures enhance the extent of oil recovery from micropores, small pores, and mesopores as well as reduce CO_2 consumption ratio. However, this study only focuses on small-scale fractured core huff-n-puff experiments. Future research should focus on larger-scale experiments, more complex fracture networks, and the use of numerical simulations or improved laboratory hydraulic fracturing techniques to better understand and replicate the effects of real hydraulic fracture geometries on CO_2 huff-n-puff performance.

(2) The oil recovery factor of CO_2 huff-n-puff in propped fracture cores are higher than those in unpropped fracture cores. As the confining pressure increases, the oil recovery factor in fractured cores noticeably decreases. The fracture closure under pressure and the compression of the matrix pore throats lower the core apparent permeability and reduce the oil recovery factor. The reduction in oil recovery factor is more pronounced in unpropped fracture cores. When the confining pressure increases from 20 to 40 MPa, the oil recovery decreases from 34.72% to 27.61%.

(3) Based on the revised local cubic law, the apparent permeability of fractured cores is expressed in terms of the fracture aperture. As the confining pressure increases, the fracture aperture significantly decreases. Under a confining pressure of 40 MPa, the fracture aperture of unpropped fracture core reduces to 21.21 μm, and the oil recovery factor is at its lowest level. Therefore, future research should focus on the

dynamic closure process of fractures under high stress and how to maintain the fractures open for extended periods.

(4) The increase in crude oil viscosity leads to a decrease in CO_2 huff-n-puff oil recovery. When using Oil sample #3, the recovery factor decreases to 21.17%. Both temperature and pressure increases can improve the CO_2 huff-n-puff oil recovery, with temperature having a more significant impact. One of the key factors in enhancing the oil recovery of CO_2 huff-n-puff in low-permeability heavy oil reservoirs is improving the flowing capability of the heavy oil.

CRediT authorship contribution statement

Di Zhu: Writing – review & editing, Writing – original draft, Methodology, Investigation, Data curation. **Bin-Fei Li:** Writing – review & editing, Visualization, Supervision, Project administration, Methodology, Data curation, Conceptualization. **Lei Zheng:** Investigation, Data curation. **Maen M. Husein:** Writing – review & editing, Investigation, Data curation. **Zheng-Xiao Xu:** Investigation. **Bo-Liang Li:** Investigation. **Zhao-Min Li:** Writing – review & editing, Supervision, Project administration, Methodology, Investigation, Funding acquisition, Data curation.

Declaration of competing interest

The authors declare that they have no known competing financial interests or personal relationships that could have appeared to influence the work reported in this paper.

Acknowledgments

This project is supported by the Open Research Fund of State Key Laboratory of Deep Oil and Gas (No. SKLDOG2024-KFYB-14). The authors acknowledge the support received from the National Nature Science Foundation of China under Grant No. U20B6003. The authors acknowledge China Scholarship Council (CSC) for financial support. We are grateful to the Shandong Engineering Research Center of Carbon Dioxide Utilization and Storage for the assistance with our experimental research in this study. The valuable comments made by the anonymous reviewers are also sincerely appreciated.

Appendix A. Supplementary data

Supplementary data to this article can be found online at https://doi.org/10.1016/j.petsci.2024.11.015.

References

Ahamed, M., Perera, M., Elsworth, D., et al., 2021. Effective application of proppants during the hydraulic fracturing of coal seam gas reservoirs: implications from laboratory testings of propped and unpropped coal fractures. Fuel 304, 121394. https://doi.org/10.1016/j.fuel.2021.121394.

Altawati, F., Emadi, H., Khalil, R., et al., 2022. An experimental investigation of improving Wolfcamp Shale-Oil recovery using Liquid-N_2-assisted N_2 and/or CO_2 Huff-n-Puff injection technique. Fuel 324, 124450. https://doi.org/10.1016/j.fuel.2022.124450.

Bao, X., Fragoso, A., Aguilera, R., 2023. CCUS and comparison of oil recovery by huff n puff gas injection using methane, carbon dioxide, hydrogen and rich gas in shale oil reservoirs. In: SPE Canadian Energy Technology Conference. https://doi.org/10.2118/212818-MS.

Cao, C.X., Song, Z.J., Shi, Y.L., et al., 2023. Study on CO_2 huff-n-puff enhanced recovery technology for Jimsar shale oil. Special Oil Gas Reservoirs 30 (3), 106–114 (in Chinese).

Cao, X.P., Liu, Z.P., Yang, Y., et al., 2021. Study on viscosity reducer flooding technology for deep low permeability extra heavy oil reservoirs. Geofluids 1–11. https://doi.org/10.1155/2021/5597520, 2021.

Charlez, P.A., 1997. Rock Mechanics. Technip.

Cheng, C.J., Milsch, H., 2021. Hydromechanical investigations on the self-propping potential of fractures in tight sandstones. Rock Mech. 54 (10), 5407–5432. https://doi.org/10.1007/s00603-021-02500-4.

Cook, N.G., 1992. Natural joints in rock: mechanical, hydraulic and seismic behaviour and properties under normal stress. Int. J. Rock Mech. Min. Sci. Geomech. Abstracts 29 (3), 198–223. https://doi.org/10.1016/0148-9062(92)93656-5.

Dong, P.F., Puerto, M., Jian, G.Q., et al., 2018. Low-IFT foaming system for enhanced oil recovery in highly heterogeneous/fractured oil-wet carbonate reservoirs. SPE J. 23 (6), 2243–2259. https://doi.org/10.2118/184569-PA.

Fredd, C.N., McConnell, S.B., Boney, C.L., et al., 2001. Experimental study of fracture conductivity for water-fracturing and conventional fracturing applications. SPE J. 6 (3), 288–298. https://doi.org/10.2118/74138-PA.

Ghanizadeh, A., Clarkson, C., Deglint, H., et al., 2016. Unpropped/propped fracture permeability and proppant embedment evaluation: a rigorous core-analysis/imaging methodology. In: SPE/AAPG/SEG Unconventional Resources Technology Conference. https://doi.org/10.15530/URTEC-2016-2459818.

Grogan, A.T., Pinczewski, W.N., 1987. The role of molecular diffusion processes in tertiary CO_2 flooding. J. Petrol. Technol. 39 (5), 591–602. https://doi.org/10.2118/12706-PA.

Guo, T.K., Zhang, S.C., Gao, J., et al., 2013. Experimental study of fracture permeability for stimulated reservoir volume (SRV) in shale formation. Transport Porous Media 98, 525–542. https://doi.org/10.1007/s11242-013-0157-7.

Huang, Y.C., Zhou, X., Zeng, F.H., 2016. Comparison study of two different methods on the localised Enkf on SAGD Processes. In: International Petroleum Technology Conference. https://doi.org/10.2523/IPTC-18907-MS.

Jia, P., Ma, M., Cao, C., et al., 2022. Capturing dynamic behavior of propped and unpropped fractures during flowback and early-time production of shale gas wells using a novel flow-geomechanics coupled model. J. Petrol. Sci. Eng. 208, 109412. https://doi.org/10.1016/j.petrol.2021.109412.

Kamali, A., Pournik, M., 2016. Fracture closure and conductivity decline modeling–Application in unpropped and acid etched fractures. J. Unconven. Oil Gas Res. 14, 44–55. https://doi.org/10.1016/j.juogr.2016.02.001.

Khatib, A.K., Earlougher, R., Kantar, K., 1981. CO_2 injection as an immiscible application for enhanced recovery in heavy oil reservoirs. In: SPE Western Regional Meeting. https://doi.org/10.2118/9928-MS.

King Jr., H.E., Eberle, A.P., Walters, C.C., et al., 2015. Pore architecture and connectivity in gas shale. Energy Fuels 29 (3), 1375–1390. https://doi.org/10.1021/ef502402e.

Kolditz, O., 2001. Non-linear flow in fractured rock. Int. J. Numer. Methods Heat Fluid Flow 11 (6), 547–575. https://doi.org/10.1108/EUM0000000005668.

Li, B.F., Bai, H., Li, A.S., et al., 2019. Experimental investigation on influencing factors of CO_2 huff and puff under fractured low-permeability conditions. Energy Sci. Eng. 7, 1621–1631. https://doi.org/10.1002/ese3.376.

Li, L., Zheng, J.Y., Shi, Y., et al., 2024a. Mechanisms of fluid migration and CO_2 storage in low permeability heavy oil reservoirs using high-pressure microfluidic CO_2 flooding experiment. Energy Fuels 38 (9), 7997–8008. https://doi.org/10.1021/acs.energyfuels.4c00869.

Li, S.Y., Lu, C., Wu, M.X., et al., 2020a. New insight into CO_2 huff-n-puff process for extraheavy oil recovery via viscosity reducer agents: an experimental study. J. CO_2 Util. 42, 101312. https://doi.org/10.1016/j.jcou.2020.101312.

Li, S.Y., Wang, Q., Zhang, K.Q., et al., 2020b. Monitoring of CO_2 and CO_2 oil-based foam flooding processes in fractured low-permeability cores using nuclear magnetic resonance (NMR). Fuel 263, 116648. https://doi.org/10.1016/j.fuel.2019.116648.

Li, S.Y., Sun, L., Wang, L., et al., 2022. Hybrid CO_2-N_2 huff-n-puff strategy in unlocking tight oil reservoirs. Fuel 309, 122198. https://doi.org/10.1016/j.fuel.2021.122198.

Li, Z., Hao, J.T., Lu, Y., et al., 2024b. Host-Guest recognition strengthened supramolecular preformed particle gel for conformance control in low-permeability fractured reservoirs. J. Mol. Liq. 412. https://doi.org/10.1016/j.molliq.2024.125893.

Liu, P.C., Wu, Y.B., Li, X.L., 2013. Experimental study on the stability of the foamy oil in developing heavy oil reservoirs. Fuel 111, 12–19. https://doi.org/10.1016/j.fuel.2013.03.021.

Lu, C., Lu, Y., Gou, X.H., et al., 2020. Influence factors of unpropped fracture conductivity of shale. Energy Sci. Eng. 8 (6), 2024–2043. https://doi.org/10.1002/ese3.645.

Lu, C., Luo, Y., Guo, J.C., et al., 2022. Numerical investigation of unpropped fracture closure process in shale based on 3D simulation of fracture surface. J. Petrol. Sci. Eng. 208, 109299. https://doi.org/10.1016/j.petrol.2021.109299.

Lv, W., Gong, H.J., Dong, M.Z., et al., 2024. Potential of nonionic polyether surfactant-assisted CO_2 huff-n-puff for enhanced oil recovery and CO_2 storage in ultra-low permeability unconventional reservoirs. Fuel 359, 130474. https://doi.org/10.1016/j.fuel.2023.130474.

Melzer, L.S., 2012. Carbon dioxide enhanced oil recovery (CO_2 EOR): factors involved in adding carbon capture, utilization and storage (CCUS) to enhanced oil recovery. Center Clim. Energy Soluti. 1–17.

Ojha, S., Bisaria, H., Mohanty, S., et al., 2024. Fractographic analysis of fiber-reinforced polymer laminate composites for marine applications: a comprehensive review. Polym. Compos. https://doi.org/10.1002/pc.28271.

Or, C., Sasaki, K., Sugai, Y., et al., 2016. Swelling and viscosity reduction of heavy oil by CO_2-gas foaming in immiscible condition. SPE Reservoir Eval. Eng. 19 (2), 294–304. https://doi.org/10.2118/179738-PA.

Pyrak-Nolte, L.J., Morris, J.P., 2000. Single fractures under normal stress: the relation between fracture specific stiffness and fluid flow. Int. J. Rock Mech. Min. Sci. 37

(1–2), 245–262. https://doi.org/10.1016/S1365-1609(99)00104-5.
Qian, K., Yang, S.L., Dou, H.E., et al., 2020. Microscopic characteristics of oil displacement with different CO_2 injection modes in extra-low permeability reservoirs. Xinjing Pet. Geol. 41 (2), 204 (in Chinese).
Ribeiro, L.H., Li, H., Bryant, J.E., et al., 2017. Use of a CO_2-hybrid fracturing design to enhance production from unpropped-fracture networks. SPE Prod. Oper. 32 (1), 28–40. https://doi.org/10.2118/173380-PA.
Sayegh, S.G., Maini, B.B., 1984. Laboratory evaluation of the CO_2 huff-n-puff process for heavy oil reservoirs. J. Can. Pet. Technol. 23 (3). https://doi.org/10.2118/84-03-02.
Sharma, M.M., Manchanda, R., 2015. The role of induced un-propped (IU) fractures in unconventional oil and gas wells. In: SPE Annual Technical Conference and Exhibition. https://doi.org/10.2118/174946-MS.
Sheng, J.J., Hayes, R.E., Maini, B.B., et al., 1999. Modelling foamy oil flow in porous media. Transport Porous Media 35, 227–258. https://doi.org/10.1023/A:1006523526802.
Snow, D.T., 1969. Closure to "rock fracture spacings, openings, and porosities." J. Soil Mech. Found Div. 95 (3), 880–883. https://doi.org/10.1061/JSFEAQ.0001290.
Sun, Y.X., Zhang, W.J., Tian, J.L., et al., 2023. Research progress on displacement mechanism of supercritical CO_2 in low-permeability heavy oil reservoir and improvement mechanism of displacement agents. Molecules 28 (16), 6154. https://doi.org/10.3390/molecules28166154.
Tharanivasan, A.K., Yang, C.D., Gu, Y.G., 2006. Measurements of molecular diffusion coefficients of carbon dioxide, methane, and propane in heavy oil under reservoir conditions. Energy Fuels 20 (6), 2509–2517. https://doi.org/10.1021/ef060080d.
Wan, T., Wang, X.J., Jing, Z.Y., et al., 2020. Gas injection assisted steam huff-n-puff process for oil recovery from deep heavy oil reservoirs with low-permeability. J. Petrol. Sci. Eng. 185, 106613. https://doi.org/10.1016/j.petrol.2019.106613.
Wang, H.Y., Sharma, M.M., 2018. Estimating unpropped-fracture conductivity and fracture compliance from diagnostic fracture-injection tests. SPE J. 23 (5), 1648–1668. https://doi.org/10.2118/189844-PA.
Wang, J., Huang, Y.X., Zhang, Y., et al., 2020. Study of fracturing fluid on gel breaking performance and damage to fracture conductivity. J. Petrol. Sci. Eng. 193, 107443. https://doi.org/10.1016/j.petrol.2020.107443.
Wang, Z.J., Li, S.Y., Li, Z.M., et al., 2023. Oil and gas pathway to net-zero: review and outlook. Energy. Strateg. Rev. 45, 101048. https://doi.org/10.1016/j.esr.2022.101048.
Wei, B., Gao, K., Song, T., et al., 2020a. Nuclear-magnetic-resonance monitoring of mass exchange in a low-permeability matrix/fracture model during CO_2 cyclic injection: a mechanistic study. SPE J. 25 (1), 440–450. https://doi.org/10.2118/199345-PA.
Wei, B., Zhong, M.Y., Gao, K., et al., 2020b. Oil recovery and compositional change of CO_2 huff-n-puff and continuous injection modes in a variety of dual-permeability tight matrix-fracture models. Fuel 276, 117939. https://doi.org/10.1016/j.fuel.2020.117939.
Wei, B., Zhong, M.Y., Tang, H.R., et al., 2021. Mass transport and exchange inside tight matrix-fracture systems during CO_2 huff-n-puff and flooding processes. In: International Petroleum Technology Conference. https://doi.org/10.2523/IPTC-21830-MS.
Xie, B., Ren, L., Jia, J.B., et al., 2020. Experimental evaluation of the self-supporting fracture conductivity for the volume fracturing in volcanic rocks. Pet. Geol. Oilfield Dev. Daqing 39 (6), 77–84 (in Chinese).
Yu, H.Y., Xu, H., Fu, W.R., et al., 2021. Extraction of shale oil with supercritical CO_2: effects of number of fractures and injection pressure. Fuel 285, 118977. https://doi.org/10.1016/j.fuel.2020.118977.
Yu, W., Lashgari, H., Sepehrnoori, K., et al., 2014. Simulation study of CO_2 huff-n-puff process in Bakken tight oil reservoirs. In: SPE Western North American and Rocky Mountain Joint Meeting. https://doi.org/10.2118/169575-MS.
Yu, W., Lashgari, H.R., Wu, K., et al., 2015. CO_2 injection for enhanced oil recovery in Bakken tight oil reservoirs. Fuel 159, 354–363. https://doi.org/10.1016/j.fuel.2015.06.092.
Yuan, Q.W., Zhou, X., Zeng, F.H., et al., 2017a. Effects of concentration-dependent diffusion on mass transfer and frontal instability in solvent-based processes. In: SPE Canada Heavy Oil Conference. https://doi.org/10.2118/184994-MS.
Yuan, Q.W., Zhou, X., Zeng, F.H., et al., 2017b. Nonlinear simulation of miscible displacements with concentration-dependent diffusion coefficient in homogeneous porous media. Chem. Eng. Sci. 172, 528–544. https://doi.org/10.1016/j.ces.2017.07.009.
Zhang, G., Tian, Y., Li, Y.J., 2019. Numerical study on the mechanism of fluid flow through single rough fractures with different JRC. Sci. Sinica Phys. Mechan. Astrono. 49 (1), 30–39 (in Chinese).
Zhang, M.Y., Li, B.F., Lei, W.S., et al., 2024. Oil displacement and CO_2 storage during CO_2 immiscible huff-n-puff within a saturated reservoir: an experimental study. Fuel 371, 132026. https://doi.org/10.1016/j.fuel.2024.132026.
Zhang, W., Wang, C.G., Guo, T.K., et al., 2021a. Study on the cracking mechanism of hydraulic and supercritical CO_2 fracturing in hot dry rock under thermal stress. Energy 221, 119886. https://doi.org/10.1016/j.energy.2021.119886.
Zhang, X., Wei, B., You, J.Y., et al., 2021b. Characterizing pore-level oil mobilization processes in unconventional reservoirs assisted by state-of-the-art nuclear magnetic resonance technique. Energy 236, 121549. https://doi.org/10.1016/j.energy.2021.121549.
Zhao, F.L., Su, W., Hou, J.R., et al., 2018. Experimental study on feasibility and mechanisms of N_2/CO_2 huff-n-puff in the fractured-cavity reservoir. Arabian J. Geosci. 11, 660. https://doi.org/10.1007/s12517-018-3993-5.
Zheng, L., 2023. Research on the Mechanism of CO_2 Fracturing-Flooding to Enhance Oil Recovery in Low Permeability Reservoirs. China University of Petroleum (East China). (in Chinese).
Zhou, B.B., Kang, W.L., Li, X.X., et al., 2024. Synergistic thickening mechanism of surfactants and supramolecular inclusion systems. J. Mol. Liq. 413. https://doi.org/10.1016/j.molliq.2024.125902.
Zhou, L., Shen, Z.H., Wang, J.D., et al., 2019a. Numerical investigating the effect of nonuniform proppant distribution and unpropped fractures on well performance in a tight reservoir. J. Petrol. Sci. Eng. 177, 634–649. https://doi.org/10.1016/j.petrol.2019.02.086.
Zhou, X., Li, X.L., Shen, D.H., et al., 2022. CO_2 huff-n-puff process to enhance heavy oil recovery and CO_2 storage: an integration study. Energy 239, 122003. https://doi.org/10.1016/j.energy.2021.122003.
Zhou, X., Yuan, Q.W., Peng, X.L., et al., 2018. A critical review of the CO_2 huff 'n'puff process for enhanced heavy oil recovery. Fuel 215, 813–824. https://doi.org/10.1016/j.fuel.2017.11.092.
Zhou, X., Yuan, Q.W., Rui, Z.H., et al., 2019b. Feasibility study of CO_2 huff'n'puff process to enhance heavy oil recovery via long core experiments. Appl. Energy 236, 526–539. https://doi.org/10.1016/j.apenergy.2018.12.007.
Zhu, C., Guo, W., Wang, Y., et al., 2021. Experimental study of enhanced oil recovery by CO_2 huff-n-puff in shales and tight sandstones with fractures. Petrol. Sci. 18 (3), 852–869. https://doi.org/10.1007/s12182-020-00538-7.
Zhu, D., Li, B.F., Chen, L.K., et al., 2024. Experimental investigation of CO_2 foam flooding-enhanced oil recovery in fractured low-permeability reservoirs: core-scale to pore-scale. Fuel 362, 130792. https://doi.org/10.1016/j.fuel.2023.130792.
Zhu, D., Li, B.F., Zheng, L., et al., 2023. Effects of CO_2 and surfactants on the interface characteristics and imbibition process in low-permeability heavy oil reservoirs. Colloids Surf., A 657, 130538. https://doi.org/10.1016/j.colsurfa.2022.130538.